MAJOR PAPER

Transient Respiratory-motion Artifact and Scan Timing during the Arterial Phase of Gadoxetate Disodium-enhanced MR Imaging: The Benefit of Shortened Acquisition and Multiple Arterial Phase Acquisition

Shintaro Ichikawa[1], Utaroh Motosugi[1,2*], Kazuyuki Sato[3], Tatsuya Shimizu[1],
Tetsuya Wakayama[4], and Hiroshi Onishi[1]

Purpose: To investigate whether shortened acquisition or multiple arterial phase acquisition improves image quality of the arterial phase compared with conventional protocol.

Methods: This retrospective study was approved by the relevant Institutional Review Board. A total of 615 consecutive patients who underwent gadoxetate disodium-enhanced MRI including one of the following three sequences in three different periods were included: (i) conventional liver acquisition with volume acceleration (LAVA) (between October 2014 and January 2015, $n = 149$), (ii) Turbo-LAVA (between March and August 2016, $n = 216$), and (iii) differential sub-sampling with Cartesian ordering (DISCO) (between January and September 2015, $n = 250$). We monitored the respiratory bellows waveform during breath holding for each patient and recorded breath-hold fidelity of the patients. Two radiologists independently evaluated the degree of respiratory artifact and scan timing on the arterial phase and compared them between the three protocols (i.e., conventional LAVA, Turbo-LAVA, and DISCO), with conventional LAVA as control.

Results: The ratio of patients with breath-hold failure was not significantly different among the three protocols ($P = 0.6340$ and 0.1085). Respiratory artifact was significantly lower in DISCO than in conventional LAVA ($P = 0.0424$), while there was no significant difference between Turbo-LAVA and conventional LAVA ($P = 0.2593$). The ratio of adequate scan timing and diagnosable image defined as no or mild artifact and adequate scan timing were higher in DISCO than in conventional LAVA ($P = 0.0025$ and 0.0019), while there was no significant difference between Turbo-LAVA and conventional LAVA ($P = 0.0780$ and 0.0657).

Conclusion: Compared with conventional protocol, multiple arterial phase acquisition (DISCO) obtained a higher number of diagnosable images by reducing respiratory motion artifact and optimizing the scan timing of arterial phase.

Keywords: *magnetic resonance imaging, artifacts, liver, image reconstruction, gadoxetate disodium*

[1]Department of Radiology, University of Yamanashi, Chuo, Yamanashi, Japan
[2]Department of Diagnostic Radiology, Kofu Kyoritsu Hospital, Kofu, Yamanashi, Japan
[3]Division of Radiology, University of Yamanashi Hospital, Chuo, Yamanashi, Japan
[4]MR Collaboration and Development, GE Healthcare, Tokyo, Japan

*Corresponding author: Department of Radiology, University of Yamanashi, 1110, Shimokato, Chuo, Yamanashi 409-3898, Japan. Phone: +81-55-273-1111, Fax: +81-55-273-6744, E-mail: umotosugi@nifty.com

Introduction

Gadoxetate disodium is a liver-specific contrast agent that allows both dynamic study and liver-specific hepatocyte imaging. Gadoxetate disodium is used worldwide for clinical liver MRI because of its high performance in lesion detection and characterization.[1–5] However, there are several reports that the transient respiratory motion artifact in the arterial phase is observed more frequently in gadoxetate disodium-enhanced MRI than in other gadolinium contrast agent-enhanced MRI.[6–8] This artifact causes nondiagnostic image quality on the arterial phase. McClellan et al.[9] reported that the maximal duration of hepatic arterial phase breath holding

was reduced after gadoxetate disodium administration in healthy volunteers. Therefore, a shorter acquisition time in the arterial phase might be a solution for this artifact. The arterial phase is typically obtained with 3D spoiled gradient recalled echo (SPGR) sequence (e.g., liver acquisition with volume acceleration [LAVA]) with >15 s breath-holding. Meanwhile, Turbo-LAVA is a modified LAVA sequence based on 3D SPGR sequence that can reduce acquisition time through the following factors: 2D parallel imaging method by auto-calibrating reconstruction for Cartesian sampling, denser data sampling performed around the center of the k-space, and the optimization of magnetic field gradient pulse.[10–12]

Another strategy for transient respiratory motion artifact is multiple arterial phase acquisition. It could provide at least one image set with reduced or no artifact. Differential subsampling with Cartesian ordering (DISCO) is a high spatiotemporal-resolution dynamic contrast-enhanced MRI technique that combines a dual-echo SPGR sequence with pseudorandom variable density k-space segmentation and view-sharing reconstruction. The DISCO technique samples an elliptically ordered central k-space region every time and subsamples the outer regions with pseudorandom segmentation to obtain aliasing artifacts from subsampling incoherence.[13]

Scan timing of arterial phase is another concern in gadoxetate disodium-enhanced MRI. The injection volume of gadoxetate disodium is half of that of extracellular gadolinium contrast agents, which indicates a short duration when using the same injection rate. DISCO could provide at least one image set with adequate scan timing on the arterial phase. Some reports showed that multiple arterial phase imaging could reduce transient respiratory motion artifact and obtain adequate scan timing on arterial phase.[14–19] However, it is still unknown which acquisitions would be the best solution to obtain optimal arterial phase images by avoiding transient respiratory motion. Thus, this study aimed to examine whether Turbo-LAVA or DISCO improves image quality by reducing respiratory motion artifact and optimizing scan timing of arterial phase compared with conventional LAVA.

Materials and Methods

Patients
This single-center, retrospective, cross-sectional study was approved by the relevant Institutional Review Board. The requirement for obtaining written informed patient consent was waived due to the retrospective nature of the study. A total of 615 consecutive patients [404 men and 211 women; mean age, 68.6 ± 10.4 (range, 22–91) years; mean body weight, 60.0 ± 12.6 (range, 31–116) kg] who underwent gadoxetate disodium-enhanced MRI including one of the following three sequences in three different periods were included in this study: (i) conventional LAVA (between October 2014 and January 2015, $n = 149$), (ii) Turbo-LAVA (between March and August 2016, $n = 216$), and (iii) DISCO (between January and September 2015, $n = 250$).

Arterial phase imaging
Gadoxetate disodium-enhanced MRI was performed using a 3.0T MR system (Discovery MR750; GE Healthcare, Chicago, IL, USA) with a 32-channel phased-array coil. Gadoxetate disodium (0.025 mmol/kg body weight) was administered at a rate of 1 mL/s followed by a 20-mL saline flush by using a power injector. DISCO was started 30 s after the start of contrast administration. We obtained multiple arterial phase (six phases) images within a single breath-hold with oxygen inhalation (acquisition time, 24 s; temporal resolution, ~4 s). In conventional LAVA and Turbo-LAVA, arterial phase images were acquired 20–30 s after the start of administration of gadoxetate disodium. Scan timing was adjusted using the fluoroscopic triggering technique. The acquisition time was 16 s for conventional LAVA and 10 s for Turbo-LAVA. Table 1 presents the scan parameters of each sequence in detail. Breath-hold status was assessed by either of the two

Table 1 Scan parameters of each sequence

	Conventional LAVA	Turbo-LAVA	DISCO
Plane	Axial	Axial	Axial
TR/TE (ms)	3.4/1.4	4.8/1.3	3.9/1.1 and 2.2
Flip angle (°)	12	15	15
FOV (mm)	340	340	340
Matrix	256 × 192	320 × 192	320 × 192
Section thickness (mm)	3.6	3.6	3.6
Intersectional gap (mm)	1.8	1.8	1.8
Number of slices	60	60	60
Bandwidth (kHz)	100	166.7	166.7
Acceleration factor	Phase 2.0/slice 1.5	Phase 2.0/slice 2.0	Phase 2.0/slice 1.5
Acquisition time (s)	16	10	24

DISCO, differential sub-sampling with Cartesian ordering; LAVA, liver acquisition with volume acceleration.

trained MR technologists using respiratory bellows monitors for precontrast and arterial phase acquisitions. Breath-hold status was classified as success (i.e., a straight or slowly varying trace during the image acquisition [Fig. 1, left]) or failure (i.e., a jagged trace during the image acquisition or the onset of sudden pronounced oscillations [Fig. 1, right]).

Image interpretation

Two independent radiologists (S.I. and T.S., with 12 and 6 years of clinical experience in abdominal MRI, respectively) who were blinded to the clinical data performed qualitative analyses of arterial phase imaging. For each dataset, they evaluated respiratory artifact using a 4-point visual score (1, no artifact; 2, mild = respiratory artifact is present but not interfering with the depiction of intrahepatic structures; 3, moderate = respiratory artifact is present and interfering with the depiction of intrahepatic structures; 4, severe = non-diagnostic images with marked artifact) (Fig. 2). Further, they evaluated whether the scan timing of the arterial phase imaging was adequate or not. Adequate timing was defined as images with appropriate enhancement of hepatic artery and portal vein without enhancement of hepatic vein (Fig. 3). Taking these two factors into account, we defined images that show no or mild respiratory artifact and adequate scan timing as diagnosable images. Reviewers first picked up the phases with adequate timing (or, in the absence of adequate timing, the phases that were considered closest to adequate timing) and evaluated the phases with the fewest respiratory artifact among them. Discrepancies between reviewers were resolved by consensus review, and
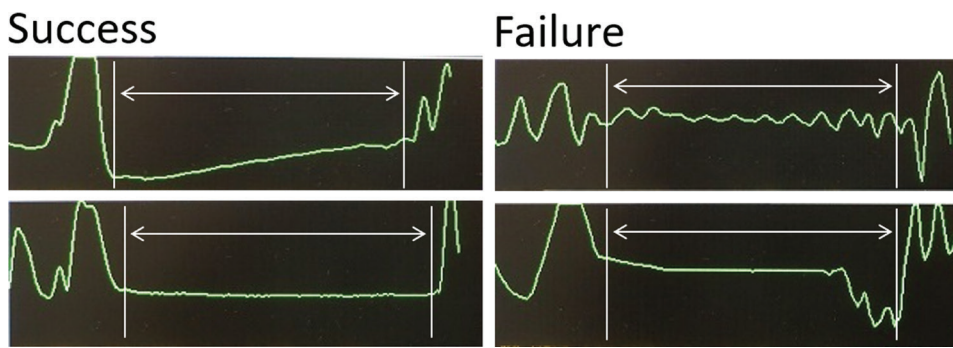

Fig. 1 Classification of breath-hold status. Breath-hold status was assessed by using respiratory bellows monitors for precontrast and arterial phase acquisitions. Breath-hold success was defined as a straight or slowly varying trace during the image acquisition (left). Breath-hold failure was defined as a jagged trace during the image acquisition or the onset of sudden pronounced oscillations (right).
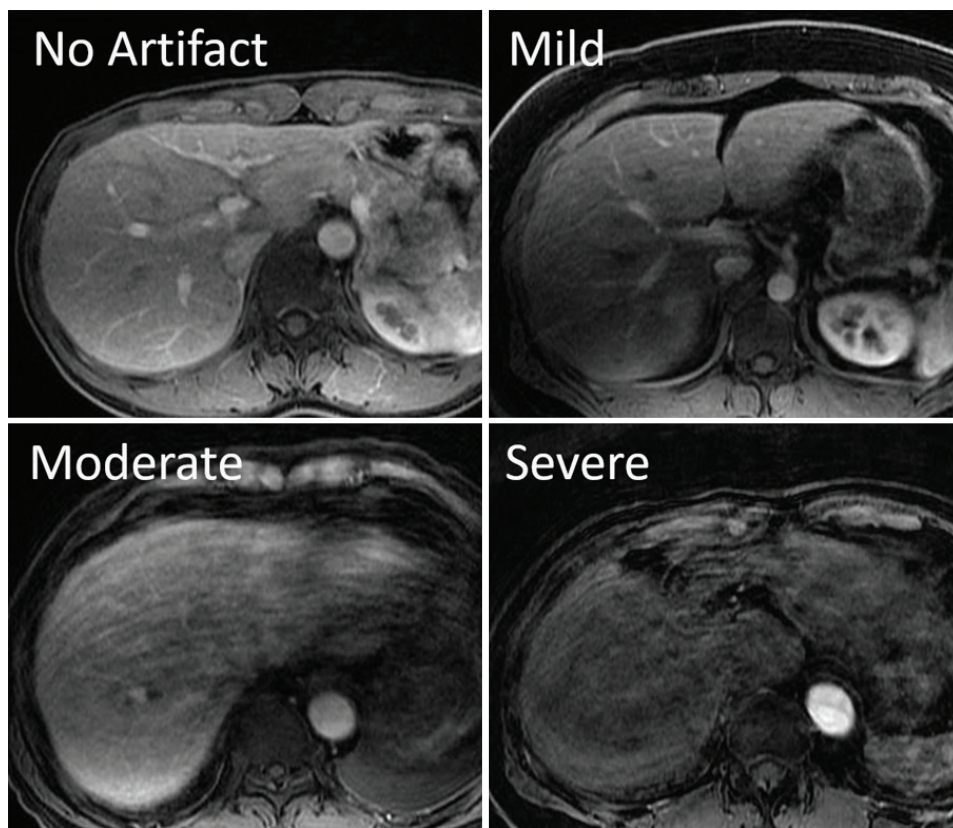

Fig. 2 Sample images of respiratory artifact grading. Respiratory artifact was assessed using a 4-point visual score (1, no artifact; 2, mild = respiratory artifact is present but not interfering with the depiction of intrahepatic structures; 3, moderate = respiratory artifact is present and interfering with the depiction of intrahepatic structures; 4, severe = non-diagnostic images with marked artifact).

Fig. 3 Sample images of scan timing of arterial phase grade. Scan timing of arterial phase was assessed as adequate or not. Adequate timing was defined as images with appropriate enhancement of hepatic artery and portal vein (arrow) without enhancement of hepatic vein (dotted arrow). Too early [without enhancement of portal vein (arrow)] and too late [enhancement of hepatic vein (dotted arrow)] scan timing were considered as inadequate scan timing.

the consensus data were used for analysis. Original data from the independent review were used to calculate interobserver agreement.

Statistical analyses
The patient characteristics were analyzed using Kruskal-Wallis and χ^2-tests. The visual assessment findings were compared for all patients and for cases of breath-hold failure using the χ^2-test with conventional LAVA set as control. Risk factor for transient respiratory motion artifact-matched cases were randomly selected and compared with conventional LAVA set as control. Cohen's kappa values were calculated to assess interobserver agreement. Agreement was considered excellent for kappa values (κ) >0.8, good for >0.6 and ≤0.8, moderate for >0.4 and ≤0.6, fair for >0.2 and ≤0.4, and poor for $\kappa \leq 0.2$. All statistical analyses were performed using JMP software (version 15.0.0; SAS Institute, Cary, NC, USA). P-values <0.05 were considered statistically significant.

Results

Patient demographics of each sequence
A significant difference between the sequences was observed in the ratio of patients with chronic liver disease ($P = 0.0174$). The underlying liver disease in these patients is shown in Table 2. Other factors including age, sex, body weight, body mass index, and in the ratio of patients with obstructive pulmonary disease and previous episodes of transient respiratory motion artifact did not show significant difference between the protocols ($P = 0.4171–0.9730$, Table 2). In the comparison among risk factor (in the ratio of patients with chronic liver disease, obstructive pulmonary disease and previous episodes of transient respiratory motion artifact-matched cases, all factors did not show significant difference between the protocols ($P = 0.7271–1.0000$, Table 3).

Qualitative image analysis
The proportion of breath-hold failure cases was not significantly different between the sequences ($P = 0.6340$ and 0.1085). The proportion of no or mild artifact, adequate scan timing, and diagnosable images were significantly higher in DISCO than in conventional LAVA ($P = 0.0019–0.0424$), while they were not significantly different between Turbo-LAVA and conventional LAVA ($P = 0.0657–0.2593$, Table 4).

Similar results were observed in the analysis focused on the breath-hold failure cases (Table 5). There were 52 and 21 breath-hold failure cases identified in DISCO and conventional LAVA, respectively. Of these, DISCO obtained diagnosable images in 71.2% (37/52) of cases, whereas conventional LAVA obtained only 33.3% (7/21) ($P = 0.0039$). There was no significant difference in the proportion of diagnosable image between Turbo-LAVA (50.0% [13/26]) and conventional LAVA ($P = 0.3742$, Table 5 and Fig. 4). Similar results were observed in the comparison among risk factor-matched cases (Tables 6 and 7). Example of images in each acquisition sequence are shown in Fig. 5.

Interobserver agreements were excellent for the respiratory artifact ($\kappa = 0.8464$ [95% CI, 0.7751–0.9178]). Meanwhile, interobserver agreements were good for the scan timing of arterial phase and diagnosable images ($\kappa = 0.6945$ [0.5612–0.8278] and 0.7780 [0.7054–0.8507], respectively). A representative case sample is shown in Fig. 6. This patient showed breath-hold failure, but diagnosable images were obtained by using DISCO.

Discussion

This retrospective study compared the image quality considering respiratory artifact and scan timing of arterial phase in gadoxetate disodium-enhanced MRI using Turbo-LAVA or

Table 2 Patient characteristics in all cases according to the MRI sequence

	Conventional LAVA	Turbo-LAVA	DISCO	P
Number of patients	149	216	250	
Age (years)	69.3 ± 9.5	68.6 ± 10.3	68.0 ± 11.1	0.8468
Sex (men:women)	99:50	141:75	164:86	0.9730
Body weight (kg)	59.8 ± 13.6	60.0 ± 12.3	60.3 ± 12.4	0.7439
Body mass index (kg/m^2)	23.2 ± 3.9	23.1 ± 3.5	23.3 ± 3.6	0.7717
Chronic liver disease	123/149 (82.6%)	152/216 (70.4%)	194/250 (77.6%)	0.0174[*]
Hepatitis C	75	71	110	
Hepatitis B	21	34	48	
Hepatitis B + C	0	2	0	
Alcoholic	12	23	23	
NASH	1	4	5	
Others[†]	14	18	8	
None	26	64	56	
Obstructive pulmonary disease	11/149 (7.4%)	13/216 (6.0%)	14/250 (5.6%)	0.7686
Episodes of transient respiratory motion artifact	14/149 (9.4%)	15/216 (6.9%)	26/250 (10.4%)	0.4171

[*]$P < 0.05$. [†]Others include primary biliary cholangitis, autoimmune hepatitis, idiopathic portal hypertension, and undetermined cause. Continuous variables were analyzed using Kruskal–Wallis test and are expressed as mean ± standard deviation. Categorical variables were analyzed using the χ^2-test and are expressed as ratios or percentage with numerators and denominators. DISCO, differential sub-sampling with Cartesian ordering; LAVA, liver acquisition with volume acceleration; NASH, non-alcoholic steatohepatitis.

Table 3 Patient characteristics in risk factor-matched cases according to the MRI sequence

	Conventional LAVA	Turbo-LAVA	DISCO	P
Number of patients	149	149	149	
Age (years)	69.3 ± 9.5	69.2 ± 9.9	68.6 ± 10.6	0.9869
Sex (men:women)	99:50	100:49	105:44	0.7271
Body weight (kg)	59.8 ± 13.6	60.2 ± 12.2	60.2 ± 12.5	0.7747
Body mass index (kg/m^2)	23.2 ± 3.9	23.0 ± 3.3	23.2 ± 3.7	0.9389
Chronic liver disease	123/149 (82.6%)	123/149 (82.6%)	123/149 (82.6%)	1.0000
Obstructive pulmonary disease	11/149 (7.4%)	11/149 (7.4%)	11/149 (7.4%)	1.0000
Episodes of transient respiratory motion artifact	14/149 (9.4%)	14/149 (9.4%)	14/149 (9.4%)	1.0000

Continuous variables were analyzed using Kruskal–Wallis test and are expressed as mean ± standard deviation. Categorical variables were analyzed using the χ^2-test and are expressed as ratios or percentage with numerators and denominators. DISCO, differential sub-sampling with Cartesian ordering; LAVA, liver acquisition with volume acceleration; NASH, non-alcoholic steatohepatitis.

Table 4 Image quality in all cases of the three sequences

	Conventional LAVA	Turbo-LAVA	DISCO
Breath-hold failure	21/149 (14.1%)	26/216 (12.0%)	52/250 (20.8%)
P-value	Control	0.6340	0.1085
No or mild artifact	127/149 (85.2%)	193/216 (89.4%)	230/250 (92.0%)
P-value	Control	0.2593	0.0424[*]
Adequate scan timing	136/149 (91.3%)	207/216 (95.8%)	245/250 (98.0%)
P-value	Control	0.0780	0.0025[*]
Diagnosable image	117/149 (78.5%)	186/216 (86.1%)	225/250 (90.0%)
P-value	Control	0.0657	0.0019[*]

[*]$P < 0.05$. Data of Turbo-LAVA and DISCO were compared with those of conventional LAVA using the χ^2-test. Categorical variables are expressed as percentage with numerators and denominators. DISCO, differential sub-sampling with Cartesian ordering; LAVA, liver acquisition with volume acceleration.

Table 5 Image quality in all cases of the three sequences in breath-hold failure cases

	Conventional LAVA	Turbo-LAVA	DISCO
No or mild artifact	7/21 (33.3%)	13/26 (50.0%)	37/52 (71.2%)
P-value	Control	0.3742	0.0039*
Adequate scan timing	19/21 (90.5%)	24/26 (92.3%)	52/52 (100%)
P-value	Control	0.8230	0.0240*
Diagnosable image	7/21 (33.3%)	13/26 (50.0%)	37/52 (71.2%)
P-value	Control	0.3742	0.0039*

*$P < 0.05$. Data of Turbo-LAVA and DISCO were compared with those of conventional LAVA using the χ^2-test. Categorical variables are expressed as percentage with numerators and denominators. DISCO, differential sub-sampling with Cartesian ordering; LAVA, liver acquisition with volume acceleration.
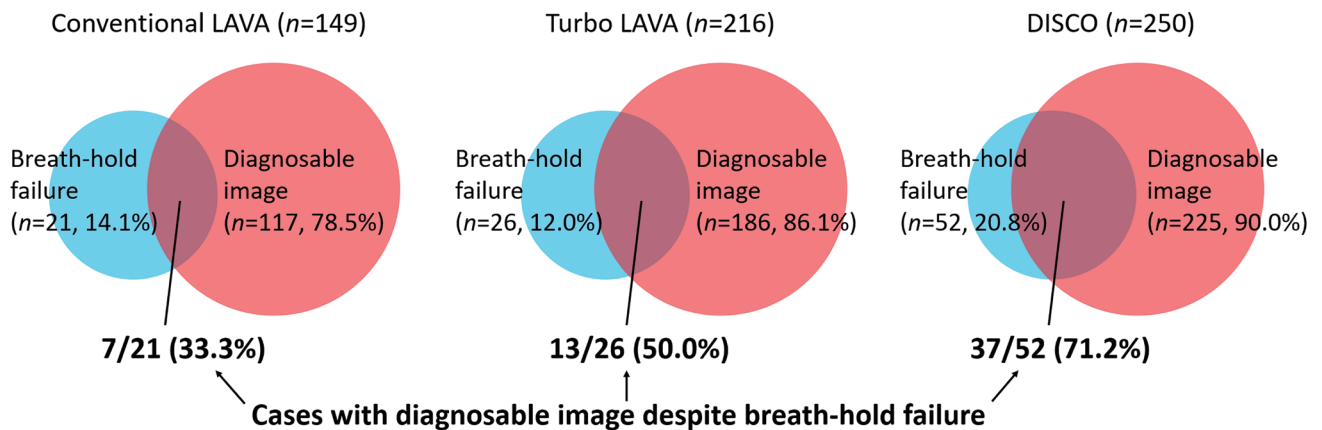

Fig. 4 Relationship between breath-hold failure and diagnosable image in each sequence. Diagram shows overlap of breath-holding failure and diagnosable image. In DISCO, diagnosable images were obtained in 71.2% (37/52) of breath-hold failure cases, while in conventional LAVA, diagnosable images were obtained in only 33.3% (7/21) of breath-hold failure cases. In Turbo-LAVA, diagnosable images were obtained in 50.0% (13/26) of breath-hold failure cases. DISCO, differential sub-sampling with Cartesian ordering; LAVA, liver acquisition with volume acceleration.

Table 6 Image quality in risk factor-matched cases of the three sequences

	Conventional LAVA	Turbo-LAVA	DISCO
Breath-hold failure	21/149 (14.1%)	21/149 (14.1%)	28/149 (18.8%)
P-value	Control	1.000	0.3485
No or mild artifact	127/149 (85.2%)	132/149 (88.6%)	139/149 (93.3%)
P-value	Control	0.4925	0.0382*
Adequate scan timing	136/149 (91.3%)	142/149 (95.3%)	148/149 (99.3%)
P-value	Control	0.2466	0.0014*
Diagnosable image	117/149 (78.5%)	127/149 (85.2%)	136/149 (90.0%)
P-value	Control	0.1755	0.0032*

*$P < 0.05$. Data of Turbo-LAVA and DISCO were compared with those of conventional LAVA using the χ^2-test. Categorical variables are expressed as percentage with numerators and denominators. DISCO, differential sub-sampling with Cartesian ordering; LAVA, liver acquisition with volume acceleration.

Table 7 Image quality in risk factor-matched cases of the three sequences in breath-hold failure cases

	Conventional LAVA	Turbo-LAVA	DISCO
No or mild artifact	7/21 (33.3%)	11/21 (52.4%)	20/28 (71.4%)
P-value	Control	0.3499	0.0105*
Adequate scan timing	19/21 (90.5%)	19/21 (90.5%)	28/28 (100%)
P-value	Control	1.0000	0.1786
Diagnosable image	7/21 (33.3%)	11/21 (52.4%)	20/28 (71.4%)
P-value	Control	0.3499	0.0105*

*$P < 0.05$. Data of Turbo-LAVA and DISCO were compared with those of conventional LAVA using the χ^2-test. Categorical variables are expressed as percentage with numerators and denominators. DISCO, differential sub-sampling with Cartesian ordering; LAVA, liver acquisition with volume acceleration.
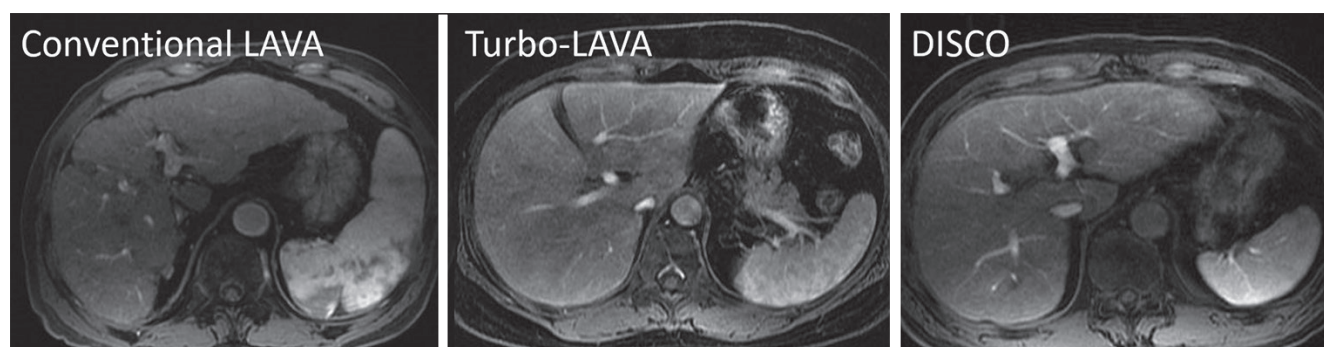

Fig. 5 Example of images in each acquisition sequence. Arterial phase images obtained by conventional LAVA (66-year-old man with hepatitis C, left), Turbo-LAVA (66-year-old woman with hepatitis C, middle), and DISCO (67-year-old man with hepatitis B, right). All of them show no respiratory artifact and adequate scan timing defined as diagnosable images. DISCO, differential sub-sampling with Cartesian ordering; LAVA, liver acquisition with volume acceleration.

DISCO and conventional LAVA. Our results revealed that compared with conventional LAVA, Turbo-LAVA does not obtain more diagnosable images. In our protocol, acquisition time of Turbo-LAVA (10 s) was 37.5% shorter than that of conventional LAVA (16 s); however, cases of breath-hold failure and respiratory artifact did not significantly decrease. That is, breath-hold failure still occurred at a similar rate despite the shortened acquisition time. Thus, Turbo-LAVA might be insufficient as a countermeasure to the transient respiratory motion artifact. This result differs from the previous report that demonstrated the short breath-hold MR technique showed better arterial phase image quality with less degraded and a lower incidence of breath-hold difficulty compared with the conventional breath-hold technique.[20] The discrepancy between our results and previous report may be due to the different definition of breath-hold failure. They defined gadoxetic acid-related dyspnea as when the standard deviation value of respiratory waveforms of the arterial phase was 200 greater than that of the precontrast phase, while we defined breath-hold failure as a jagged trace during the image acquisition or the onset of sudden pronounced oscillations of respiratory waveforms. Therefore, it is possible that milder breath-hold difficulty cases may be included in our study. Moreover, they evaluated overall

image quality for arterial phase, while we defined images that show no or mild respiratory artifact and adequate scan timing as diagnosable images. This difference in evaluation methods may also have contributed to the differences in results. Meanwhile, we found that compared with conventional LAVA, DISCO obtained diagnosable images in more patients by reducing respiratory motion artifact and optimizing scan timing of the arterial phase. This result was also observed in subgroup analysis of patients with breath-hold failure. Although there was no significant difference in the proportion of breath-hold failure cases between DISCO and conventional LAVA, respiratory motion artifact was decreased and scan timing was optimized in DISCO. This result suggests that even in breath-hold failure cases, multiple arterial phase acquisition can obtain at least one diagnosable image set.

Several approaches have been reported to reduce transient respiratory motion artifact; these include gadoxetate disodium diluted with saline,[21] training of patients for modified breathing command by the responsible technician,[22] or oxygen inhalation in patients with a prior episode of transient respiratory motion artifact.[23] However, it is impossible to completely avoid transient respiratory motion artifact in the arterial phase of gadoxetate disodium-enhanced MRI.
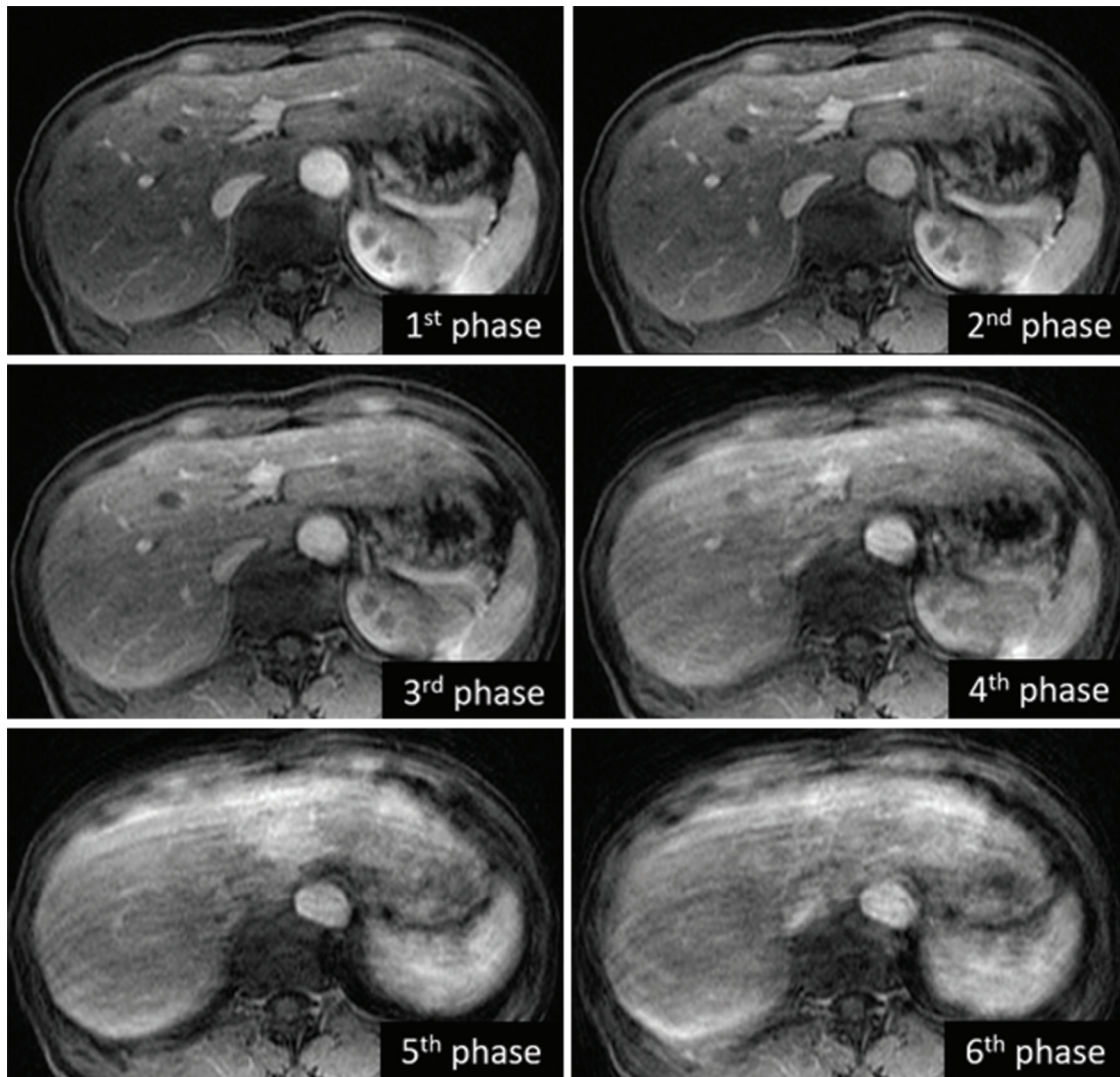
Fig. 6 Representative magnetic resonance images of the breath-hold failure case. A 63-year-old woman with hepatitis C showed breath-hold failure. Various grades of respiratory motion artifacts were observed in DISCO sequence (mild in third phase, moderate in fourth phase, and severe in fifth and sixth phases). However, diagnosable images (no or mild artifact and adequate scan timing of arterial phase) were obtained in the first, second, and third phases. DISCO, differential sub-sampling with Cartesian ordering.

Among various solutions, several studies reported that multiple arterial phase acquisition is a promising technique to obtain at least one or two diagnosable image sets.[15–19] Our results were consistent with these reports. However, one study showed that multiple arterial phase acquisition failed to reduce transient respiratory motion artifact compared with single arterial phase.[24] The differences might be caused by the different backgrounds of target patients or the sample sizes. Several potential risk factors of transient severe motion can also influence the results, including age, sex, body mass index, pulmonary disease, and previous episodes of transient respiratory motion artifact.[6,25–28] However, these risk factors vary between studies.[28,29] In addition, the type of the view sharing technique may also be influenced the differences. The previous report applied either 4D time-resolved angiography with keyhole (4D-TRAK) or time-resolved imaging with interleaved stochastic trajectories (TWIST) on multiple arterial phase acquisition.[24] In the 4D-TRAK, central k-space is sampled repeatedly in a random manner, while peripheral k-space is acquired once to serve as a reference scan for each reconstruction. Thus, motion artifact may be also shared on all of the arterial phase images, if transient respiratory motion artifact occurred.

Another benefit of multiple arterial phase acquisition is that it enables adequate scan timing for arterial phase. In our study, the proportion of adequate scan timing in DISCO was significantly higher than that in conventional LAVA, consistent with previous reports.[14,24] This finding supports that multiple arterial phase acquisition is useful to achieve adequate scan timing for the arterial phase. However, our study also shows that even with the multiple arterial phase acquisition, scan timing can still be inadequate (2.0% [5/250]). To

address this issue, continuous acquisition with retrospective reconstruction for multiple dynamic contrast-enhanced MRI is necessary. Radial *k*-space sampling technique can be a potential solution to completely address breath-hold failure and inadequate scan timing in arterial phase imaging.[30]

Our study has some limitations. First, this study was retrospective without any randomization. However, our routine protocols for liver MRI were changed from conventional LAVA to DISCO and then to Turbo-LAVA over time. Therefore, selection bias was negligible because the patients were not intentionally selected. Second, we did not evaluate the diagnostic performance for focal hepatic lesions. Although we believe that DISCO and Turbo-LAVA could show high diagnostic performance, further studies are needed to determine whether DISCO or Turbo-LAVA can replace conventional LAVA.

Conclusion

In summary, compared with conventional LAVA, DISCO obtained a higher rate of diagnosable image by reducing respiratory motion artifact and optimizing scan timing of the arterial phase. Meanwhile, there was no difference in the ratio of diagnosable image between conventional LAVA and Turbo-LAVA.

Conflicts of Interest

The co-author Tetsuya Wakayama is an employee of GE Healthcare. The other authors declare that they have no conflicts of interest.

References

1. Kim SS, Kim SH, Song KD, Choi SY, Heo NH. Value of gadoxetic acid-enhanced MRI and diffusion-weighted imaging in the differentiation of hypervascular hyperplastic nodule from small (<3 cm) hypervascular hepatocellular carcinoma in patients with alcoholic liver cirrhosis: a retrospective case-control study. J Magn Reson Imaging 2020; 51:70–80.
2. Moon JY, Kim SH, Choi SY, Hwang JA, Lee JE, Lee J. Differentiating malignant from benign hyperintense nodules on unenhanced T_1-weighted images in patients with chronic liver disease: using gadoxetic acid-enhanced and diffusion-weighted MR imaging. Jpn J Radiol 2018; 36:489–499.
3. Vanhooymissen IJSML, Thomeer MG, Braun LMM, et al. Intrapatient comparison of the hepatobiliary phase of Gd-BOPTA and Gd-EOB-DTPA in the differentiation of hepatocellular adenoma from focal nodular hyperplasia. J Magn Reson Imaging 2019; 49:700–710.
4. Nakao S, Tanabe M, Okada M, et al. Liver imaging reporting and data system (LI-RADS) v2018: comparison between computed tomography and gadoxetic acid-enhanced magnetic resonance imaging. Jpn J Radiol 2019; 37:651–659.
5. Li J, Wang J, Lei L, Yuan G, He S. The diagnostic performance of gadoxetic acid disodium-enhanced magnetic resonance imaging and contrast-enhanced multi-detector computed tomography in detecting hepatocellular carcinoma: a meta-analysis of eight prospective studies. Eur Radiol 2019; 29:6519–6528.
6. Motosugi U, Bannas P, Bookwalter CA, Sano K, Reeder SB. An investigation of transient severe motion related to gadoxetic acid-enhanced MR imaging. Radiology 2016; 279:93–102.
7. Furlan A, Close ON, Borhani AA, Wu YH, Heller MT. Respiratory-motion artefacts in liver MRI following injection of gadoxetate disodium and gadobenate dimeglumine: an intra-individual comparative study in cirrhotic patients. Clin Radiol 2017; 72:93.e1–93.e6.
8. Ikeno H, Kobayashi S, Kozaka K, et al. Relationship between the degree of abdominal wall movement and the image quality of contrast-enhanced MRI: semi-quantitative study especially focused on the occurrence of transient severe motion artifact. Jpn J Radiol 2020; 38:165–177.
9. McClellan TR, Motosugi U, Middleton MS, et al. Intravenous gadoxetate disodium administration reduces breath-holding capacity in the hepatic arterial phase: a multi-center randomized placebo-controlled trial. Radiology 2017; 282:361–368.
10. Brau AC, Beatty PJ, Skare S, Bammer R. Comparison of reconstruction accuracy and efficiency among autocalibrating data-driven parallel imaging methods. Magn Reson Med 2008; 59:382–395.
11. Low RN, Bayram E, Panchal NJ, Estkowski L. High-resolution double arterial phase hepatic MRI using adaptive 2D centric view ordering: initial clinical experience. AJR Am J Roentgenol 2010; 194:947–956.
12. Hori M, Kim T, Onishi H, et al. Single-breath-hold thin-slice gadoxetic acid-enhanced hepatobiliary MR imaging using a newly developed three-dimensional fast spoiled gradient-echo sequence. Magn Reson Imaging 2016; 34:545–551.
13. Saranathan M, Rettmann DW, Hargreaves BA, Clarke SE, Vasanawala SS. DIfferential Subsampling with Cartesian Ordering (DISCO): a high spatio-temporal resolution Dixon imaging sequence for multiphasic contrast enhanced abdominal imaging. J Magn Reson Imaging 2012; 35:1484–1492.
14. Gruber L, Rainer V, Plaikner M, Kremser C, Jaschke W, Henninger B. CAIPIRINHA-Dixon-TWIST (CDT)-VIBE MR imaging of the liver at 3.0T with gadoxetate disodium: a solution for transient arterial-phase respiratory motion-related artifacts? Eur Radiol 2018; 28:2013–2021.
15. Xiao YD, Ma C, Liu J, Li HB, Zhou SK, Zhang ZS. Transient severe motion during arterial phase in patients with Gadoxetic acid administration: can a five hepatic arterial subphases technique mitigate the artifact? Exp Ther Med 2018; 15:3133–3139.
16. Li H, Xiao Y, Wang S, et al. TWIST-VIBE five-arterial-phase technology decreases transient severe motion after bolus injection of Gd-EOB-DTPA. Clin Radiol 2017; 72:800. e1–800.e6.
17. Pietryga JA, Burke LM, Marin D, Jaffe TA, Bashir MR. Respiratory motion artifact affecting hepatic arterial phase imaging with gadoxetate disodium: examination recovery

with a multiple arterial phase acquisition. Radiology 2014; 271:426–434.

18. Grazioli L, Faletti R, Frittoli B, et al. Evaluation of incidence of acute transient dyspnea and related artifacts after administration of gadoxetate disodium: a prospective observational study. Radiol Med 2018; 123:910–917.

19. Sofue K, Marin D, Jaffe TA, Nelson RC, Bashir MR. Can combining triple-arterial phase acquisition with fluoroscopic triggering provide both optimal early and late hepatic arterial phase images during gadoxetic acid-enhanced MRI? J Magn Reson Imaging 2016; 43:1073–1081.

20. Yoo JL, Lee CH, Park YS, et al. The short breath-hold technique, controlled aliasing in parallel imaging results in higher acceleration, can be the first step to overcoming a degraded hepatic arterial phase in liver magnetic resonance imaging: a prospective randomized control study. Invest Radiol 2016; 51:440–446.

21. Polanec SH, Bickel H, Baltzer PAT, et al. Respiratory motion artifacts during arterial phase imaging with gadoxetic acid: can the injection protocol minimize this drawback? J Magn Reson Imaging 2017; 46:1107–1114.

22. Gutzeit A, Matoori S, Froehlich JM, et al. Reduction in respiratory motion artefacts on gadoxetate-enhanced MRI after training technicians to apply a simple and more patient-adapted breathing command. Eur Radiol 2016; 26:2714–2722.

23. Namimoto T, Shimizu K, Nakagawa M, et al. Reducing artifacts of gadoxetate disodium-enhanced MRI with oxygen inhalation in patients with prior episode of arterial phase motion: intra-individual comparison. Clin Imaging 2018; 52:11–15.

24. Min JH, Kim YK, Kang TW, et al. Artifacts during the arterial phase of gadoxetate disodium-enhanced MRI: multiple arterial phases using view-sharing from two different vendors versus single arterial phase imaging. Eur Radiol 2018; 28:3335–3346.

25. Shah MR, Flusberg M, Paroder V, Rozenblit AM, Chernyak V. Transient arterial phase respiratory motion-related artifact in MR imaging of the liver: an analysis of four different gadolinium-based contrast agents. Clin Imaging 2017; 41:23–27.

26. Hayashi T, Saitoh S, Tsuji Y, et al. Influence of gadoxetate disodium on oxygen saturation and heart rate during dynamic contrast-enhanced MR imaging. Radiology 2015; 276:756–765.

27. Davenport MS, Bashir MR, Pietryga JA, Weber JT, Khalatbari S, Hussain HK. Dose-toxicity relationship of gadoxetate disodium and transient severe respiratory motion artifact. AJR Am J Roentgenol 2014; 203:796–802.

28. Bashir MR, Castelli P, Davenport MS, et al. Respiratory motion artifact affecting hepatic arterial phase MR imaging with gadoxetate disodium is more common in patients with a prior episode of arterial phase motion associated with gadoxetate disodium. Radiology 2015; 274:141–148.

29. Well L, Rausch VH, Adam G, Henes FO, Bannas P. Transient severe motion artifact related to gadoxetate disodium-enhanced liver MRI: frequency and risk evaluation at a German Institution. Rofo 2017; 189:651–660.

30. Yoon JH, Lee JM, Yu MH, et al. Evaluation of transient motion during gadoxetic acid-enhanced multiphasic liver magnetic resonance imaging using free-breathing golden-angle radial sparse parallel magnetic resonance imaging. Invest Radiol 2018; 53:52–61.